Geophysical Research Letters

Supporting Information for

Monsoonal forcing of European ice-sheet dynamics during the Late Quaternary

Stefanie Kaboth-Bahr[1,2], André Bahr[2], Christian Zeeden[3], Samuel Toucanne[4], Frederique Eynaud[5], Francisco Jiménez-Espejo[6], Ursula Röhl[7], Oliver Friedrich[2], Jörg Pross[2], Ludvig Löwemark[1], Lucas J. Lourens[8]

[1] Department of Geosciences, National Taiwan University, Taipei City 106, Taiwan

[2] Institute of Earth Sciences, Heidelberg University, 69210 Heidelberg, Germany

[3] IMCEE, Observatoire de Paris, PSL Research University, Paris 75014, France

[4] Ifremer, Centre Bretagne, UR Geosciences Marines, Plouzané Cedex 29280, France

[5] Université de Bordeaux, Pessac Cedex 33607, France

[6] JAMSTEC, Yokosuka-city 237-0061, Japan

[7] MARUM, University of Bremen, 28359 Bremen, Germany

[8] Department of Earth Sciences, Utrecht University, Utrecht 3584CD, The Netherlands

Contents of this file

S1. Imprint of glacial EIS variations on global sea level reconstructions

According to numerical ice sheet models, the EIS contributed approximately 35 m of sea level equivalent, i.e. ~33%, to the global ice volume that build-up during the LGM compared to modern-day level (de Boer et al., 2014). However, the estimated impact of

EIS variability on the intra-glacial sea level variations was rather minuscule. Volume flux estimates for the Fleuve Manche meltwater discharge events during the last glaciation range between 0.01–0.4 Sv (Toucanne et al., 2010). These values are similar to the amounts of meltwater released during Heinrich Events (0.1–0.4 Sv; Hemming, 2004; Roche et al., 2004). Considering that a meltwater release of 0.29 Sv equals a sea level increase of a 2±1 m (Roche et al., 2004), this yields a maximum of ~3 m sea level increase during Fleuve Manche events. This amplitude is below the accumulated uncertainty of sea level reconstructions based on the stable oxygen isotope composition of benthic foraminifera which amounts to ±10 m (de Boer et al., 2014). Hence, sea level fluctuations induced by EIS build-up and melting during MIS 2-4 do not feature significantly in the LR04 global benthic stack.

S2. Hydrographic setting at Site U1389 (Gulf of Cadiz)

At its water depth of 630 m, IODP Site U1389 is directly influenced by the core of the upper Mediterranean Outflow water (MOW; Hernández-Molina et al., 2013). The warm, highly saline MOW (~13°C, >36 PSU; Fig. DR1) is a unique feature of the depth interval between 550 to 1200 m in the Eastern North Atlantic (Ambar and Howe, 1979). It is directly fed by saline intermediate-water masses that exit the Mediterranean Sea through the Strait of Gibraltar and subsequently cascade down the water column due their high density (Millot, 2014). The water column above the MOW is dominated by North Atlantic Central water of subtropical (14–16 C and ~36.2 PSU;) and subpolar origin (~13 C and ~35.9 PSU; Peliz et al., 2009, 2005; Fig. S1).

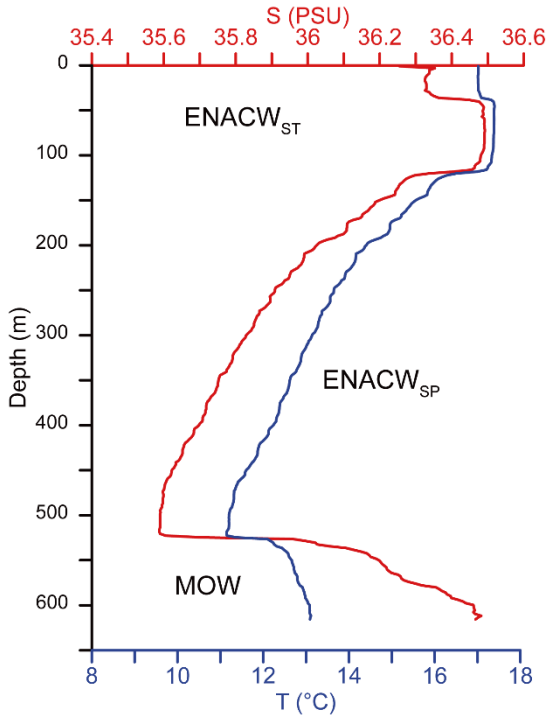

Figure S1: Modern water-mass structure at Site U1389 derived from World Ocean Atlas 2013 (Boyer et al., 2013). The red line represents the temperature profile, whereas the blue line represents salinity. MOW = Mediterranean Outflow Water; ENACW$_{SP}$ = North Atlantic Central Water of subpolar origin; ENACW$_{ST}$ = North Atlantic Central Water of subtropical origin.

S3. Mediterranean-Atlantic exchange and the evolution of MOW

Today, the water-mass exchange between the eastern North Atlantic and the Mediterranean Sea is driven by the density contrast of its water masses (Rogerson et al., 2012). The dense water forming in the Mediterranean Sea is both warmer and saltier (~13.4 °C; 38.4 psu) than the North Atlantic Central Water (NACW; 11.4 to 12.5 °C; 35.6 to 35.7 psu). Dense Mediterranean-sourced water moves westward into the North Atlantic through the lower 100 m of the Strait of Gibraltar, while North Atlantic water flows eastward through the upper part (~200 m) of the strait into the Mediterranean Sea (Ambar & Howe, 1979; Bryden

et al., 1994; Bryden & Stommel, 1984). Due to its narrowness, the dense water accelerates to speeds of approximately ~1 m/s and a volume transport of ~1 Sv at Spartel West sill (Baringer & Price, 1997). Because the flow is subcritical, the ~300 m deep Strait of Gibraltar does not confine the volume flux (Rogerson et al., 2012). At Spartel West sill, the dense MOW enters the Atlantic Ocean, descends along the continental slope and accelerates along the steeper part of the slope to a maximum velocity of ~1.2 m/s (Sánchez-Leal et al., 2017). Due to the higher velocity of the MOW compared to the surrounding NACW the velocity difference generates small-scale eddies (Baringer & Price, 1997). These eddies draw less-dense ambient water into the current, which increases its volume flux (from ~1 Sv at Spartel West sill to ~2.7 Sv downstream of the sill) while slowing its velocity to ~0.4 m s-1 (Sánchez-Leal et al., 2017). The MOW has been shown to entrain most of the NACW within 50 km from exiting the Strait of Gibraltar, where the velocity of the density current reaches its maximum (Baringer & Price, 1997). As a consequence of entraining NACW, the temperature of the MOW drops from 13.4 °C at the sill to 12.45 °C, and its salinity is reduced from 38.4 psu to 36.45 psu, thus, decreasing its salinity when leaving the Gulf of Cadiz (Sánchez-Leal et al., 2017). These final values of water temperature and salinity determine the neutrally buoyant depth of the MOW between 600 to 1,300 m (Baringer & Price, 1997). Due to the Coriolis force the dense product water of the MOW (after NACW entrainment) banks to the right against the continental slope of the Gulf of Cádiz and divides horizontally into upper- and midslope branches which flow as a nearly geostrophic current until Cape St. Vincent. There, the salinity and temperature signature of the MOW mixes into the ambient NACW water through Meddies which

contribute to the spreading of the Mediterranean Salt Tongue within the North Atlantic water mass structure (Baringer & Price, 1997).

S4. Constraining the phase relation between MOW production and EIS dissociation

A central aspect of the proposed precession-paced relation between MOW-driven EIS build-up and subsequent ice sheet decay during increasing summer insolation is the lag of melt water delivery by the Fleuve Manche paleoriver to enhanced MOW production. In our data this temporal succession is reflected by the lag of maxima in high Ti/Ca ratios in Site MD03-2692 (i.e. high Fleuve Manche activity) to high Zr/Al of IODP Site U1389 (i.e. strong MOW production) by a half to a third of a precession cycle.

To test for the null hypothesis that both MOW production and Fleuve Manche activity are synchronous, we performed a novel optimization procedure based on the "astrochron" R software package(Meyers, 2014; R Core Team, 2014; Zeeden et al., 2015). This algorithm allows to constrain potential age model-related uncertainties that might bias our comparison of Zr/Al record from Site U1389 and Ti/Ca ratios from MD03-2692. It uses the existing age models as a starting point and allows to determine a maximum deviation of up to 12 kyr from the initial tie points. The algorithm correlates the proxy record used for tuning (i.e. planktic $\delta^{18}O$ and Zr/Al for Site U1389 and benthic $\delta^{18}O$ for Site MD03-2692) to the La2004 orbital solution (Laskar et al., 2004). Starting from the respective initial age model (cf. Methods in the main text), each simulation run (n = 650) uses different relative contributions of precession and obliquity to the La2004 orbital solution. It then calculates the correlation between input proxy record and modified orbital

110 solution. After completing the simulation runs the optimization algorithm selects
111 automatically the best fit of highest correlation.

112 The statistical testing of the initial chronologies of Sites U1389 and MD03-2692
113 yielded Pearson correlation coefficients of r^2 = 0.58 and 0.68, respectively. Utilizing
114 statistical optimization, no significant improvement of these correlation factors could be
115 achieved (r^2 = 0.48 and 0.63, respectively). The lower correlation of the optimisation
116 approach can be ascribed to the used targets. The here presented age models are correlated
117 to paleoclimate reference data, while the optimisation approach uses orbital parameters as
118 correlation target. This strongly supports the robustness of the herein used initial age
119 models. Nevertheless, the algorithm provides a statistically significant variation of the
120 initial age model which allows to analyse the influence of tuning changes on the phase
121 relation of respective proxy records, in our case the precession-paced MOW and EIS
122 dynamics.

123 To quantify the age model bias that results from applying the original and modelled
124 age model, we filtered the Zr/Al and Ti/Ca data sets of Site U1389 and MD02-2692 for
125 precession, respectively (Fig. S2). For both data sets, the average time offset of the
126 precession signal from the original and the revised age model is ±1 kyr. The potential age
127 model uncertainty on precession timescales is thus distinctly smaller than the observed ~7
128 kyr phase offset between Sites U1389 and MD03-2692. Hence, even given the age model
129 uncertainties derived from different tuning options, we conclude that the null hypothesis
130 of a synchronous MOW production and EIS disintegration can be refuted.

131 Cross-spectral analysis was carried out to test the phase relationship of our proxy
132 records representing Mediterranean Outflow variability (as reflected by the Zr/Al ratio at

Site U1389) and melt-water discharge of the European ice-sheets via the Fleuve Manche palaeoriver (reflected by the Ti/Ca ratio at Site MD03-2692). We used a cross-multi-taper algorithm implemented in the "astrochron" R software package (Meyers, 2014; R Core Team, 2014); results are consistent with the cross-B-Tukey method of AnalySeries (Paillard et al., 1996).

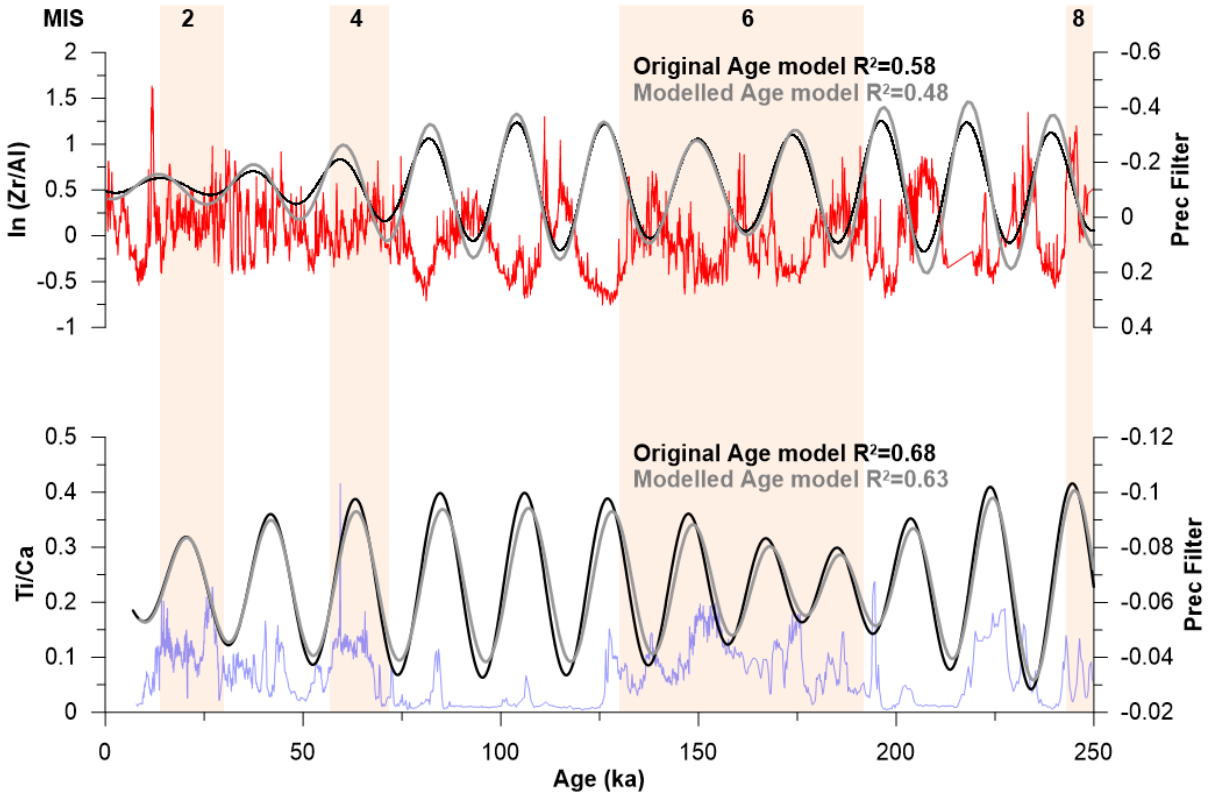

Figure S2: Differences between the initial and optimized age models of Sites U1389 and MD03-2692 within the precession band. The upper panel shows the original Zr/Al data of U1389, the lower panel the Ti/Ca record of Site MD03-2692. Superimposed are the respective filter outputs derived from the detrended data (using a Taner band pass filter, included in the "astrochron" package (Meyers, 2014) implemented in R with cut-off frequencies of 0.04 and 0.054 and a roll-off rate of $10^{\wedge 5}$). The black lines denote the filter

results of the initial age model, the grey lines the filter response of the modelled age model. Marine Isotope Stages (MIS) are indicated on top of the figure and are marked by red bars.

S5. Faunal proxies for warm water mass advection at the Iberian Margin

To reconstruct the advection of subtropical water masses along the Iberian Margin during the last 250 kyr, we evaluated the previously published relative abundance data of planktic foraminifera that are associated with the Azores Current and favour warm surface waters at Site MD95-2040 (Singh et al., 2015; Voelker and de Abreu, 2011). Following Singh et al. (2015), we utilized the surface- and near-surface-dwelling species *Globigerinoides ruber* (white and pink), *Globigerinoides sacculifer*, *G. trilobatus*, *Globoturborotalita rubescens*, and *Orbulina universa*, but excluded deep-water-dwelling species *Globorotalia truncalinoides* and *Globorotalia hirsute* (Hemleben et al., 2012).

References

Ambar, I., & Howe, M. R. (1979, May). Observations of the mediterranean outflow—II the deep circulation in the vicinity of the gulf of cadiz. *Deep Sea Research Part A. Oceanographic Research Papers*. https://doi.org/10.1016/0198-0149(79)90096-7

Baringer, M. O., & Price, J. F. (1997). Mixing and Spreading of the Mediterranean Outflow. *Journal of Physical Oceanography*. https://doi.org/10.1175/1520-0485(1997)027<1654:MASOTM>2.0.CO;2

de Boer, B., Lourens, L. J., & van de Wal, R. S. W. (2014). Persistent 400,000-year variability of Antarctic ice volume and the carbon cycle is revealed throughout the Plio-Pleistocene. *Nature Communications*, *5*. https://doi.org/10.1038/ncomms3999

Boyer, T. P., Antonov, J. I., Baranova, O. K., Coleman, C., Garcia, H. E., Grodsky, A., et al. (2013). *World Ocean Database 2013. NOAA Atlas NESDIS 73*.

Bryden, H. L., & Stommel, H. M. (1984). Liminting processes thatdetermine basic features of the circulation in the Mediterranean Sea. *Oceanologica Acta*, *7*(3), 289–296.

Bryden, H. L., Candela, J., & Kinder, T. H. (1994). Exchange through the Strait of Gibraltar. *Progress in Oceanography*. https://doi.org/10.1016/0079-6611(94)90028-0

Hemleben, C., Spindler, M., & Anderson, O. (2012). *Modern planktonic foraminifera*. Springer Science & Business Media. Retrieved from https://books.google.de/books?hl=de&lr=&id=pSLoBwAAQBAJ&oi=fnd&pg=PA1&dq=Modern+Planktonic+Foraminifera&ots=9JvXucQJuw&sig=bNQjG3RJQQY6aIKbpUjT0A6ToaQ

Hemming, S. R. (2004). Heinrich events: Massive late Pleistocene detritus layers of the North Atlantic and their global climate imprint. *Reviews of Geophysics*, *42*(1), RG1005. https://doi.org/10.1029/2003RG000128

Hernández-Molina, F. J., Stow, D., Alvarez-Zarikian, C., Acton, G., Bahr, A., Balestra, B., et al. (2013). IODP Expedition 339 in the Gulf of Cadiz and off West Iberia: Decoding the environmental significance of the Mediterranean outflow water and its global influence. *Scientific Drilling*, *16*, 1–11. https://doi.org/10.5194/sd-16-1-2013

Laskar, J., Robutel, P., Joutel, F., Gastineau, M., Correia, A. C. M., & Levrard, B. (2004). A long-term numerical solution for the insolation quantities of the Earth. *Astronomy and Astrophysics*, *428*(1), 261–285. https://doi.org/10.1051/0004-6361:20041335

Meyers, S. R. (2014). astrochron: An R Package for Astrochronology. Retrieved from

http://cran.r-project.org/package=astrochron

Millot, C. (2014). Heterogeneities of in- and out-flows in the Mediterranean Sea. *Progress in Oceanography*, *120*, 254–278. https://doi.org/10.1016/j.pocean.2013.09.007

Paillard, D., Labeyrie, L., & Yiou, P. (1996). Macintosh Program performs time-series analysis. *Eos, Transactions American Geophysical Union*, *77*(39), 379–379. https://doi.org/10.1029/96EO00259

Peliz, A., Marchesiello, P., Santos, A. M. P., Dubert, J., Teles-Machado, A., Marta-Almeida, M., & Le Cann, B. (2009). Surface circulation in the Gulf of Cadiz: 2. Inflow-outflow coupling and the Gulf of Cadiz slope current. *Journal of Geophysical Research*, *114*(C03011), 1–16. https://doi.org/10.1029/2008JC004771

Peliz, Á., Dubert, J., Santos, A. M. P., Oliveira, P. B., & Le Cann, B. (2005). Winter upper ocean circulation in the Western Iberian Basin—Fronts, Eddies and Poleward Flows: an overview. *Deep Sea Research Part I: Oceanographic Research Papers*, *52*(4), 621–646. https://doi.org/10.1016/j.dsr.2004.11.005

R Core Team. (2014). R: A language and environment for statistical computing. Vienna, Austria: R Foundation for Statistical Computing. Retrieved from http://www.r-project.org/

Roche, D., Paillard, D., & Cortijo, E. (2004). Constraints on the duration and freshwater release of Heinrich event 4 through isotope modelling. *Nature*, *432*(7015), 379–382. https://doi.org/10.1038/nature03059

Rogerson, M., Rohling, E. J., Bigg, G. R., & Ramirez, J. (2012). Paleoceanography of the Atlantic-Mediterranean exchange: Overview and first quantitative assessment of climatic forcing. *Reviews of Geophysics*, *50*(2), RG2003.

https://doi.org/10.1029/2011RG000376

Sánchez-Leal, R. F., Bellanco, M. J., Fernández-Salas, L. M., García-Lafuente, J., Gasser-Rubinat, M., González-Pola, C., et al. (2017). The Mediterranean Overflow in the Gulf of Cadiz: A rugged journey. *Science Advances*, *3*(11). https://doi.org/10.1126/sciadv.aao0609

Singh, A. D., Verma, K., Jaiswal, S., Alonso-Garcia, M., Li, B., & Abrantes, F. (2015). Planktic foraminiferal responses to orbital scale oceanographic changes off the western Iberian margin over the last 900kyr: Results from IODP site U1391. *Global and Planetary Change*, *135*, 47–56. https://doi.org/10.1016/j.gloplacha.2015.10.002

Toucanne, S., Zaragosi, S., Bourillet, J.-F., Marieu, V., Cremer, M., Kageyama, M., et al. (2010). The first estimation of Fleuve Manche palaeoriver discharge during the last deglaciation: Evidence for Fennoscandian ice sheet meltwater flow in the English Channel ca 20–18ka ago. *Earth and Planetary Science Letters*, *290*(3–4), 459–473. https://doi.org/10.1016/j.epsl.2009.12.050

Voelker, A. H. L., & de Abreu, L. (2011). A Review of Abrupt Climate Change Events in the Northeastern Atlantic Ocean (Iberian Margin): Latitudinal, Longitudinal, and Vertical Gradients. In H. Rashid, L. Polyak, & E. Mosley-Thompson (Eds.), *Abrupt Climate Change: Mechanisms, Patterns, and Impacts* (Vol. 193, pp. 15–37). Washington, D. C.: American Geophysical Union. https://doi.org/10.1029/2010GM001021

Zeeden, C., Meyers, S. R., Lourens, L. J., & Hilgen, F. J. (2015). Testing astronomically tuned age models. *Paleoceanography*, *30*(4), 369–383. https://doi.org/10.1002/2014PA002762